

Effect of the Mn-Mn exchange interaction on the high-field magnetoresistance and magnetization in n -type $\text{Hg}_{1-x-y}\text{Cd}_x\text{Mn}_y\text{Te}$

N. Yamada,* S. Takeyama, T. Sakakibara, T. Goto, and N. Miura

Institute for Solid State Physics, University of Tokyo, Roppongi, Minato-ku, Tokyo 106, Japan

(Received 23 August 1985; revised manuscript received 12 May 1986)

The magnetoresistance and the magnetization in n -type semimagnetic semiconductors $\text{Hg}_{1-x-y}\text{Cd}_x\text{Mn}_y\text{Te}$ (with $x=0.027-0.214$, $y=0.009-0.023$) have been measured in pulsed high magnetic fields up to 35 T. The magnetoresistance versus magnetic field curve displayed an anomaly at $H=15-20$ T, depending on the Mn composition. At the same magnetic field, a steplike anomaly was also observed in the magnetization. Both of these phenomena are attributed to the magnetic-field-induced alignment of the antiferromagnetically coupled nearest-neighbor Mn^{2+} ion pairs. The exchange constant J between ions in the pair was found to depend on the energy gap, varying in the range from -9.4 to -12.8 K.

I. INTRODUCTION

Recently, semimagnetic semiconductors such as $\text{Hg}_{1-x}\text{Mn}_x\text{Te}$, $\text{Cd}_{1-x}\text{Mn}_x\text{Se}$, etc., have attracted much attention for their characteristic magnetic properties as well as the influence of the s - d interaction between mobile carriers and localized magnetic moments on their transport properties. The magnetic properties of such materials can be controlled by varying the Mn composition.¹ The change in the Mn composition is accompanied by a considerable change in the band gap. In contrast, in quaternary mixed crystals like $\text{Hg}_{1-x-y}\text{Cd}_x\text{Mn}_y\text{Te}$, the energy gap can be widely varied in a controlled fashion by varying the Cd composition x , independent of the Mn composition y . This enables us to study the magnetic and the transport properties of dilute magnetic systems over a wide range of band gap without changing the Mn composition.

In metals, the interaction between randomly distributed magnetic ions has been a subject of interest for many years.² In semimagnetic semiconductors $\text{Hg}_{1-x-y}\text{Cd}_x\text{Mn}_y\text{Te}$, Mn^{2+} ions on cation sites are known to form clusters. Assuming an antiferromagnetic exchange interaction between nearest neighbors (NN's), the clusters can form a pair, an open or closed triangle, etc. The influence of the exchange interaction with the next nearest neighbors or more distant neighbors is negligibly small in comparison to the NN interaction because of the much smaller exchange constants. Clusters consisting of more than three Mn^{2+} ions can be also neglected since the existing probabilities of such clusters are very small for $y < 0.05$. At low magnetic fields, the ground state of the NN pair has zero magnetic moment, so that its energy is independent of the field. On increasing the magnetic field, the Zeeman-split energy levels of the excited states of the NN pair cross the lowest lying level. Thus discontinuous change of the magnetic moment of the lowest level is caused each time when such crossing occurs. These crossovers between the lowest level and the second lowest level at fields H_N should give rise to steplike increases in the magnetization at low temperatures.

As the temperature is increased, the steplike structure in the magnetization would be broadened because of the population in the higher energy levels. Such a steplike increase was actually observed up to $N=2$ by Shapira *et al.* for $\text{Cd}_{0.951}\text{Mn}_{0.049}\text{Se}$ and $\text{Zn}_{0.967}\text{Mn}_{0.033}\text{Se}$,³ and by Aggarwal *et al.* for $\text{Cd}_{0.95}\text{Mn}_{0.05}\text{Se}$ (Ref. 4) and $\text{Cd}_{0.95}\text{Mn}_{0.05}\text{Te}$.⁵ The values of J obtained from these measurements are -8.3 , -13 and -8.7 , -7.7 K for each crystal, respectively.

In semimagnetic semiconductors, it is an interesting question how other semiconducting properties are influenced by the level crossover which causes the magnetization anomaly. By measuring the magnetorelectance of $\text{Cd}_{1-x}\text{Mn}_x\text{Se}$ (Ref. 4) and $\text{Cd}_{1-x}\text{Mn}_x\text{Te}$,⁵ Aggarwal *et al.* succeeded in observing a steplike change in the excitation Zeeman splitting. In narrow gap or zero gap semimagnetic semiconductors, such as $\text{Hg}_{1-x}\text{Mn}_x\text{Te}$ and $\text{Hg}_{1-x-y}\text{Cd}_x\text{Mn}_y\text{Te}$, the transport properties are affected by the s - d interaction between conduction electrons and localized Mn^{2+} spins. One of the purposes of the present paper is to investigate the influence of the magnetization on the transport properties in $\text{Hg}_{1-x-y}\text{Cd}_x\text{Mn}_y\text{Te}$ by measuring both the magnetization and the magnetoresistance in high magnetic fields. It was found for the first time that the longitudinal magnetoresistance showed a slope change (kink) corresponding to the level crossover mentioned above. From the field positions of the steplike change of the magnetization or the kink of the magnetoresistance, the antiferromagnetic exchange constant J between the NN Mn^{2+} ions can be determined. For such an exchange interaction in narrow gap or zero gap semimagnetic semiconductors, an indirect exchange mechanism via virtual interband transitions may play a significant role.⁶⁻⁸ From this viewpoint, the band-gap dependence of J is studied for several samples with various x .

II. EXPERIMENTAL PROCEDURE

Quaternary single crystals of $\text{Hg}_{1-x-y}\text{Cd}_x\text{Mn}_y\text{Te}$ were grown with a modified Bridgman method.⁹ The Mn content y was kept approximately constant near 0.01. The

TABLE I. Characteristics of the measured $\text{Hg}_{1-x-y}\text{Cd}_x\text{Mn}_y\text{Te}$ samples. The band gap E_g is between the Γ_8 and Γ_6 band. The negative gap denotes the zero gap between the Γ_8 conduction and the Γ_8 valence bands, and the positive gap denotes the open gap between the Γ_6 conduction and the Γ_8 valence bands. N and $\rho(0)$ were measured at 4.2 K. * denotes not measured.

Sample	x	y	Band gap E_g (meV)	Carrier concentration n (10^{16} cm^{-3})	Fermi energy E_F (meV)	Resistivity at $H=0$ $\rho(0)$ ($10^{-4} \Omega \text{ cm}$)
No. 1 (9-12B)	0.027	0.009	-214	4.25	21.6	13.7
No. 2 (9-9B2)	0.027	0.009	-173	6.88	34.0	8.1
No. 3 (9-11A)	0.056	0.015	-146	*	*	*
No. 4 (9-11A2)	0.056	0.015	-146	3.17	25.1	47.0
No. 5 (14-2)	0.214	0.022	+181	2.24	17.9	50.6
No. 6 (5-6-2)	0.210	0.023	+181	4.65	27.8	40.0

Cd content x was varied between 0.027 and 0.214 (the corresponding energy gap is between -214 and $+181$ meV).⁹ Six samples were investigated in the present measurements and are listed in Table I. The composition of x and y was determined by an x-ray microprobe analyzer (XMA). The samples were cut from the wafers whose variation of x and y was less than 0.004 within the diameter of about 15 mm.

Pulsed high magnetic fields up to 35 T were produced by a copper wire-wound solenoid using a condenser bank of 200 kJ.¹⁰ The duration of the field was about 20 ms. The intensity of the field was measured by integrating a voltage induced in a pickup coil. The pulsed magnet was immersed in liquid nitrogen. The sample temperature could be reduced to 1.5 K by pumping on the He bath.

The transport properties were measured in pulsed high fields using standard techniques at Institute of Solid State Physics (ISSP). The rectangular samples had dimensions of about $0.5 \times 0.5 \times 7 \text{ mm}^3$. They were etched in a 5% mixture of bromine in methanol after ground with carborundum. In-10% Sn provided good Ohmic contacts which are most important to obtain a good signal-to-noise ratio for measurements in pulsed magnetic fields. The details are reported in Ref. 11.

The magnetization measurements were performed by using a circuit as shown in Fig. 1. The inner and outer detecting coils were wound in the opposite direction in such a manner that they have the same value of r^2n ; where r is the radius and n the number of turns of the inner and outer coils. By connecting these coils in series, the difference in the signals from both coils were measured. In principle, the resulting signal should be proportional to dM/dt . In reality, however, the incomplete compensation leads to a spurious signal proportional to dH/dt superimposed on the dM/dt signal. This spurious signal was canceled by mixing the dH/dt signal picked up by the compensation coil. The signals were recorded in digital memories of a transient recorder.

Since the magnetic system is very dilute in the present study, the magnetization signal is rather weak. Moreover, to observe the very small steplike change due to a NN pair which is even more dilute, the signal-to-noise ratio in the pulsed fields allowed magnetization measurements in fields up to 25 T, whereas transport measurements could be per-

formed in fields up to 35 T. For supplementary magnetization measurements at lower fields up to 15 T, a superconducting magnet was also employed.

III. EXPERIMENTAL RESULTS

A. Transport

Longitudinal and transverse magnetoresistance and the Hall effect were measured in magnetic fields up to 35 T. The carrier concentration of the samples used in the present work is of the order of 10^{16} cm^{-3} . This yields the last Shubnikov-de Haas (SdH) oscillation peak in the field range 2–7 T. At higher fields, the samples attain the quantum limit regime, and all the carriers populate the lowest Landau level.

Figure 2 shows the longitudinal magnetoresistance for sample No. 6 (see Table I). The slope of the magnetoresistance curve showed an abrupt change at 14 T, nearly the same magnetic field as the magnetization anomaly that was observed for sample No. 5. The slope change (the kink) is more readily visible in the second derivative of the longitudinal magnetoresistance with respect to the magnetic field as shown in Fig. 3. The kink shows up as a minimum in the $d^2\rho_{||}/dH^2$ curve at the position indicated by the arrows. In this sample the second anomaly H_2 was observed at 29.6 T. As H_2 is close to the high-field end

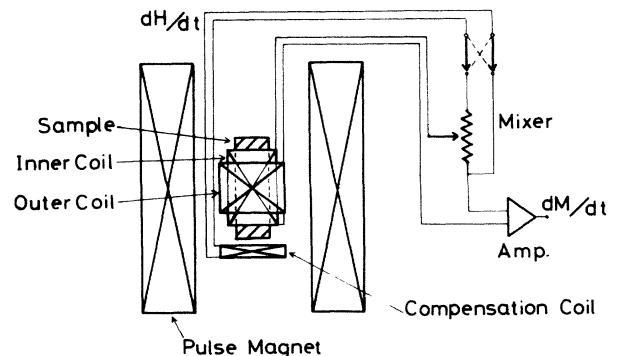


FIG. 1. Block diagram of the experimental system for the magnetization measurement in pulsed high magnetic field.

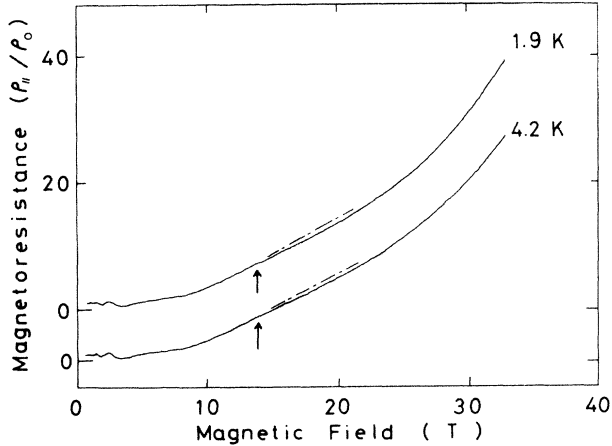


FIG. 2. Longitudinal magnetoresistance for sample No. 6 at $T=1.9$ K and $T=4.2$ K. The dot-dashed lines indicate the linear extrapolation from the low-field part of the data. At the field shown by arrows, the slope of the curve changes discontinuously.

of the measurement, there is more ambiguity as for the exact position of H_2 in comparison with that of H_1 .

Figure 4 depicts the transverse magnetoresistance and the carrier concentration, $\sigma_{xy}B/e$, for the same sample. The last SdH peak was observed at about 7 T. The curve for $\sigma_{xy}B/e$ showed a decrease with increasing field above 16 T indicating a carrier freeze-out effect. The transverse magnetoresistance is a monotonically increasing function of magnetic field. With this orientation, there is no sign of the anomaly in the region of H_1 . Furthermore, no anomalies were observed in the transverse magnetoresistance in any other samples.

Figures 5 and 6 display other examples of the longitudinal magnetoresistance and its derivative for sample No. 1. The kink is clearly seen at $H_1=16.5$ T. The first kink in the longitudinal magnetoresistance at H_1 was observed in

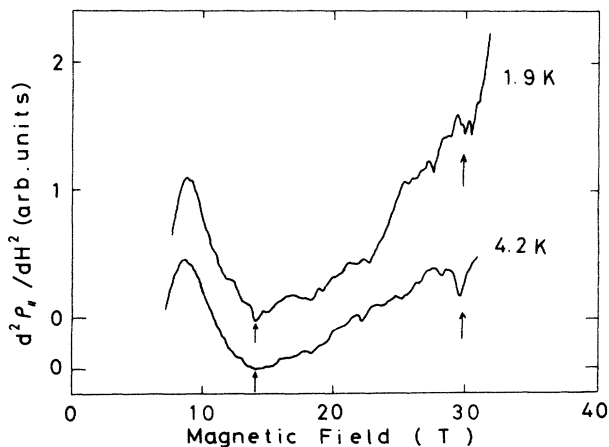


FIG. 3. Second derivative of the data shown in Fig. 2 with respect to the magnetic field for sample No. 6. At the fields pointed by arrows, minima are observed corresponding to the kink in the magnetoresistance curve.

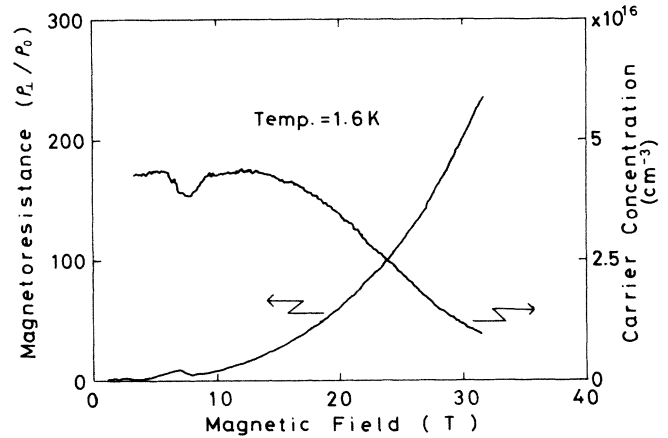


FIG. 4. Transverse magnetization ρ_1/ρ_0 and $\sigma_{xy}H/e$ (equivalent to the carrier concentration) as a function of magnetic field for sample No. 6.

all the measured samples, but the second kink at H_2 was observed only for sample No. 6, probably because H_2 was too high in other samples. The kinks in the magnetoresistance could be observed equally well in the temperature range between 1.5 and 4.2 K.

The kink has nothing to do with the quantum oscillation, since the samples are already in the quantum limit in such high fields. The origin of the kink is attributed to the crossover of the magnetic energy levels of the NN pairs of Mn^{2+} ions as will be discussed in the following sections.

B. Magnetization

The magnetization measurements were performed on samples No. 1, No. 3, and No. 5. An experimental trace of the magnetization curve obtained for sample No. 3 with a zero band gap in a pulsed field is shown in Fig. 7. It can be seen that the two traces obtained on the up-

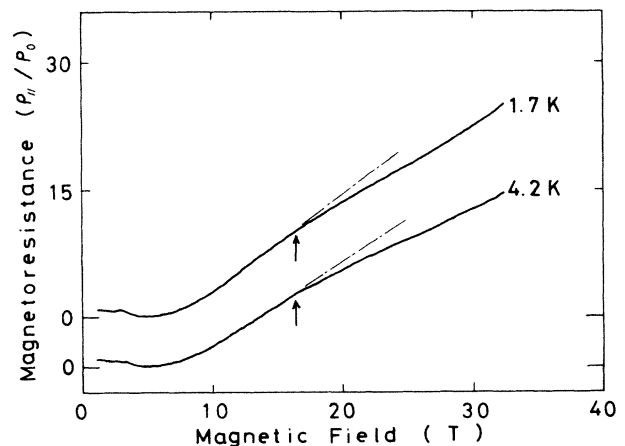


FIG. 5. Longitudinal magnetoresistance curve for sample No. 1, whose magnetization data is shown. The field H_1 is shown by arrows.

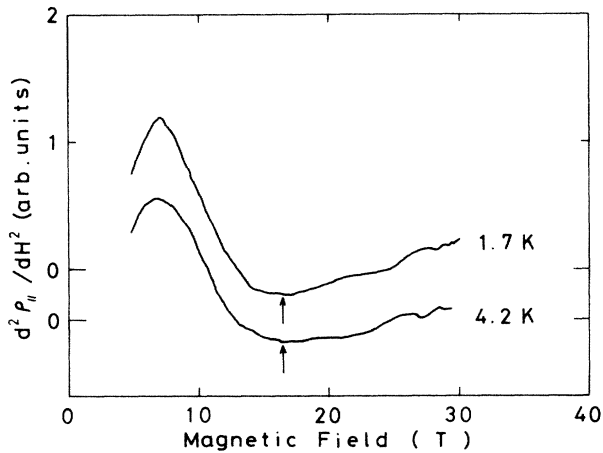


FIG. 6. Second derivative of the data shown in Fig. 5 with respect to the magnetic field for sample No. 1.

rising and down-fallig magnetic field slopes almost coincide, indicating good reproducibility of the data. The small deviation of the two traces is due to a temperature change by the adiabatic magnetization and demagnetization, which is estimated to be less than 1 K. The whole magnetization curve is almost Brillouin functionlike, but at the field shown by an arrow, a small steplike change is observed. It can be more clearly seen in the lower curve for which the vertical scale is magnified by 10 times. This corresponds to the first step at H_1 due to the level crossover as is discussed in Sec. IV. The step was observed in all the measured samples. The exact field position of the step was determined with the dM/dH curve as shown in Fig. 8 for sample No. 1. The step in the M curve shows up as a well-defined peak in the dM/dH curve.

Figure 9 shows the data for sample No. 1 which has also a zero band gap, together with a theoretical curve. Here the circles denote the experimental data and the

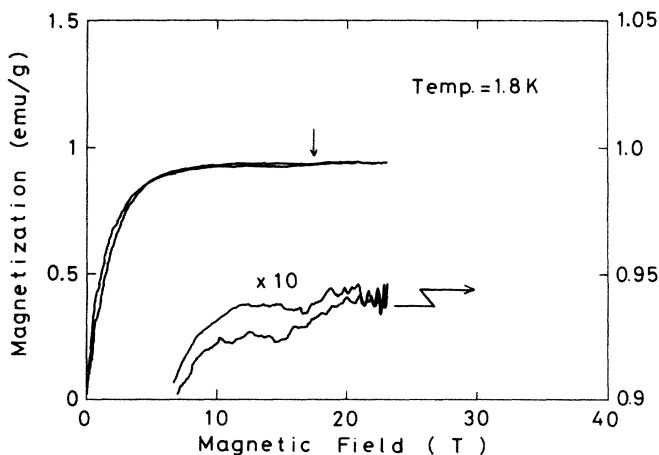


FIG. 7. Magnetization curve for sample No. 3. The vertical scale is magnified 10 times for the lower curve to show clearly the step (arrow). The temperature is 1.8 K.

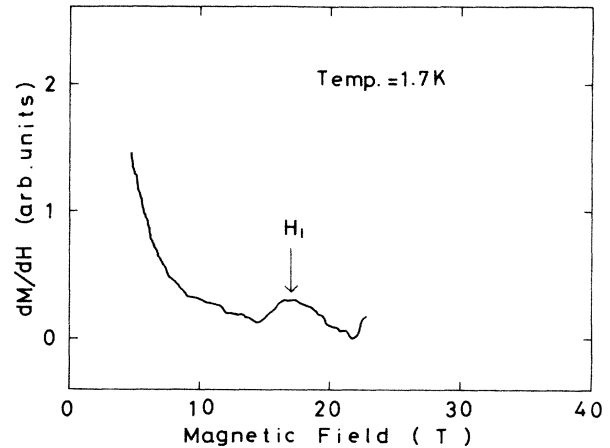


FIG. 8. Derivative of the magnetization dM/dH as a function of magnetic field for sample No. 1. The steplike change in the magnetization is observed as a peak at the field shown by an arrow.

solid lines the theoretical curve which will be discussed in Sec. IV. The agreement between theory and experiment is reasonably good both over the whole field range and in the vicinity of the step as seen in the $\times 10$ magnified curve.

For sample No. 5 with a positive gap, the measurement using a pulsed magnet was difficult because of the poor signal-to-noise ratio, so that the measurement was done with a superconducting magnet. Since the magnetic field does not cover the entire step region, it is difficult to determine the H_1 value by inspection of the dM/dH curve. Therefore, the H_1 value for this sample was determined by fitting a calculated magnetization curve to the experimental curve by adjusting H_1 as a fitting parameter.

It should be noted that the steplike increase of the magnetization and the kink of the magnetoresistance occurred at almost the same field. It was also found for other sam-

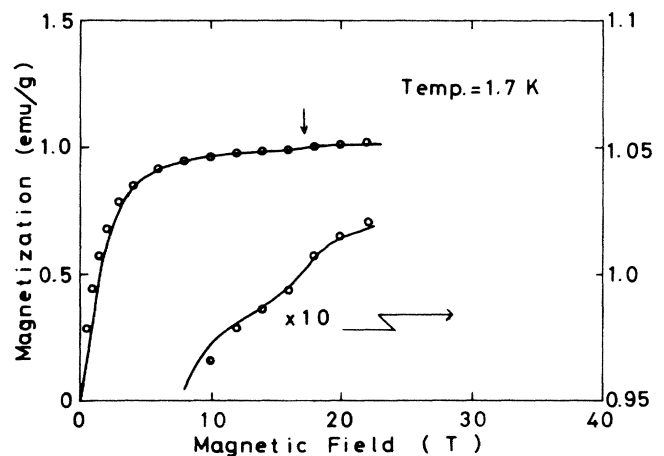


FIG. 9. Comparison between theory and experiment of the magnetization curve for sample No. 1. The solid lines represent the theoretical lines and the open circles indicate the experimental data. The vertical scale of the lower curve is magnified 10 times. The steplike change is indicated by an arrow.

field H_N , with $N=2,3,4,5$. Assuming J is independent of magnetic field, H_N is represented by

$$H_N = -NJ/\mu_B. \quad (3)$$

At magnetic fields lower than H_1 , the NN pair's lowest state is $S_T=S_z=0$. The probabilities that one can find a Mn^{2+} ion in each of the NN clusters are

$$\begin{aligned} P_s &= (1-y)^{12} \text{ for isolated spins,} \\ P_p &= 12y(1-y)^{18} \text{ for pairs.} \end{aligned} \quad (4)$$

Here the zinc-blende structure of $\text{Hg}_{1-x-y}\text{Cd}_x\text{Mn}_y\text{Te}$ is assumed. For $y < 0.03$, the probabilities for triangles are very small. The magnetization of the system below and above the first step H_1 is expressed by

$$\begin{aligned} M &= \frac{5}{2}y\bar{P}_s N_0 B_{5/2} \left(\frac{5\mu_B H}{k(T+T_0)} \right) \\ &+ \frac{1}{2}yP_p N_0 \left[1 + \exp \left(\frac{2\mu_B}{kT} (H_1 - H) \right) \right]^{-1}, \end{aligned} \quad (5)$$

where N_0 is the number of cation sites per gram, $B_{5/2}(x)$ is the Brillouin function for $S = \frac{5}{2}$, T_0 is a phenomenological parameter representing exchange interactions,^{13,14} and \bar{P}_s is the effective probability for the isolated Mn^{2+} ion concentration. \bar{P}_s is different from P_s , because of the small contributions from larger clusters, i.e., triangles, quadruplet, quintet, etc., are included in this term.

The second term in (5) represents the contribution of the NN pairs which gives rise to the first step. The magnetization for the measured samples was calculated by using (5). The calculated results are in excellent agreement with the experimental data as shown in Fig. 9 for sample No. 1. In this calculation, the values by y and T_0 were adjusted independently. In the case of sample No. 1, for example, the best fit was obtained when we assumed $y=0.0134$ and $T_0=2.5$ K. Here, $H_1=17$ T was determined from the dM/dH curve. The assumed y is slightly larger than the Mn content of the sample $y=0.009$. The reason of this discrepancy may be partly because of the error involved in the estimation of the absolute value of y by XMA and partly because of that of the absolute value of the magnetization. Good agreement between theory and experiment, as shown in Fig. 9, suggests the validity of this postulation as well as the validity of the model that the steplike change is caused by the level crossover as shown in Fig. 10.

B. Conductivity change at the level crossover

As is mentioned in Sec. IIIB, a kink was observed in the longitudinal magnetoresistance at the same field as the step was observed in the magnetization. Since this observation was confirmed in many samples with different band gaps over a wide range, it can be concluded that the kink is also associated with the level crossover as shown in Fig. 10.

Interesting questions then arise about the mechanism of the conductivity change by the level crossover, in particular, the reasons why the magnetoresistance slope decreases

for $H > H_1$, and why such a change occurs only in the longitudinal magnetoresistance and not in the transverse case.

As for the first point, a few possibilities can be considered. The first possibility is direct s - d scattering by the pairs. At the level crossover, only the magnetization of the pairs changes. The wavelength of the conduction electrons, $1/k_F$, is much larger than the size of the NN pairs, the conduction electrons would feel only the total spin of the pair S_T rather than each spin in the pair. Wittlin *et al.* investigated the spin-dependent scattering of electrons by isolated spins, and derived a relaxation time for the s - d scattering as follows:¹⁵

$$1/\tau = A[\langle S^+S^- \rangle + \langle S^-S^+ \rangle] + B[\langle S^2 \rangle - \langle S_z^2 \rangle], \quad (6)$$

where A and B are functions of E_F , H , and the band parameters. In the present case of the scattering by pairs, the same expression can be applied by replacing S_T for S . This type of s - d scattering may well cause a conductivity change at the crossover. However, at the crossover point, the first term should result in a resistance increase for $H > H_1$ in comparison to $H < H_1$. This contradicts the experimental results. The second term may give rise to a maximum around $H = H_1$ rather than a slope change.

The second possibility is the effect of weak localization. It is well known that at low temperatures, conduction electrons tend to be Anderson localized by disorder. The application of a magnetic field breaks the wave-function interference at the localization giving rise to the negative magnetoresistance.¹⁶ The alignment of the localized spin would modify the local potential fluctuation and this might weaken the localization effect. Therefore, if the spin alignment of the NN pairs takes place discontinuously at $H = H_1$, this would decrease the slope of the magnetoresistance curve. In fact, the zero-field resistance of the samples showed a small temperature dependence at low temperatures, thus electrons may well be in a weakly localized regime. However, more experimental investigation is required to justify this conjecture.

Next, we can also consider the possibility of a change of the screening length in impurity scattering.¹⁷ At low temperatures, the dominant carrier scattering mechanism is impurity scattering. If the screening length changes by the magnetization change, a steplike change of the magnetization should have an influence on the magnetoresistance. However, it is not certain by what mechanism the screening length is affected by the magnetization.

Thus the mechanism of the conductivity change at the level crossover remains unsolved. It also has to be solved why the kink in the magnetoresistance was observed even at 4.2 K, whilst the steplike change in the magnetization was observed only at lower temperatures. This fact is suggestive of a mechanism where the observed kink is directly related to the level crossover rather than indirectly via the change of magnetization. More experimental and theoretical work will be able to clarify the mechanism of this interesting phenomenon.

The reason why the kink was only observed in the longitudinal magnetoresistance is probably because the trans-

verse magnetoresistance has a steep background slope, thus the kink was obscured.

C. Band-gap dependence of the exchange constant

Finally, we discuss the exchange constant obtained in the present experiment. Table II lists the antiferromagnetic exchange constant between Mn^{2+} ions in the NN pair. The exchange constant was obtained from H_1 by using (3). The Mn^{2+} - Mn^{2+} exchange constants range between 8–13 K in these materials. Since the exchange constant depends on the distance between Mn^{2+} ions, it is not so straightforward to make a comparison among different materials with various lattice constants. However, we can investigate the band gap dependence of J among the measured $\text{Hg}_{1-x-y}\text{Cd}_x\text{Mn}_y\text{Te}$ samples which have almost the same lattice constant but different band gaps. Because of the finite experimental accuracy, it is difficult to see the difference among negative gap samples or among positive gap samples. However, the difference between the samples having band gaps with opposite signs is quite evident. Namely, the negative gap samples have $|J|$ about 2 K larger than the positive gap ones.

According to Bastard and Lewiner, the indirect exchange mechanism via an interband transition is very important for the exchange constant between two localized spins at Mn^{2+} ions in narrow or zero gap semimagnetic semiconductors.^{6,7} The RK(K)Y [Ruderman-Kittel-(Kasuya)-Yosida] interaction due to the intraband transition is negligibly small for the present case because of the small carrier concentration. Lee and Liu showed that in positive gap materials, the electron-heavy hole transitions lead to an antiferromagnetic coupling whereas the electron–light-hole transitions give rise to a ferromagnetic coupling due to band mixing effect.⁸ Because the first effect is dominant, the net exchange interaction constant, due to the interband indirect exchange mechanisms, is negative, i.e., antiferromagnetic. In negative gap crystals, on the other hand, another significant contribution comes from the interband transition between the degenerate Γ_8 valence band and Γ_8 conduction band. This gives rise to an antiferromagnetic coupling.

On the basis of these theoretical considerations, it is

reasonable that the negative gap samples have a larger $|J|$ value than the positive gap samples because of the additional Γ_8 - Γ_8 contribution. It should be noted that the difference in the exchange constants between the samples in the two regimes is ~ 2 K, which is close to the estimated value of ~ 0.2 meV (~ 2.3 K) by Bastard and Lewiner for the contribution of the Γ_8 - Γ_8 transition.⁶ A more quantitative comparison between theory and experiment is difficult because of the lack of knowledge concerning the energy band's dispersion relationship over the whole Brillouin zone, and also the background terms which arise from other contributions.

Although only the first step at H_1 was observed in the magnetization measurement, an anomaly in the longitudinal magnetoresistance corresponding to the second level crossover was observed for sample No. 1 at $H_2 = 29.6 \pm 1.0$ T. The observed position H_2 is slightly above the expected value $H_2 = 2H_1 = 28.4$ T. However, the discrepancy is within experimental error.

The discussion mentioned above is based on the assumption that the kink in the magnetoresistance arises from the same origin as the magnetization step. Although this assumption has not been verified directly, there are sufficient reasons to be led to this conjecture.

V. SUMMARY

To summarize, we have observed for the first time a steplike change in the magnetization as well as a kink in the magnetoresistance at the same magnetic field in n -type $\text{Hg}_{1-x-y}\text{Cd}_x\text{Mn}_y\text{Te}$ with various band gaps. The change in the magnetization can be interpreted in terms of a level crossover of the antiferromagnetically coupled nearest-neighbor Mn^{2+} ion pairs. The kink in the magnetoresistance is attributed to the same origin, although the mechanism of the conductivity change remains an open question. It was found that the antiferromagnetic exchange constant $|J|$ is larger for the zero gap crystals than for the positive gap crystals. This is qualitatively elucidated on the basis of an indirect exchange interaction between Mn^{2+} ions in the nearest-neighbor pairs through the different interband electron transitions.

*Present address: Department of Mathematical Engineering and Instrumentation Physics, University of Tokyo, Hongo, Tokyo 113, Japan.

¹J. K. Furdyna, *J. Appl. Phys.* **53**, 7637 (1982).

²C. Kittel, in *Solid State Physics*, edited by F. Seitz, D. Turnbull, and H. Ehrenreich (Academic, New York, 1968), Vol. 22, p. 1.

³Y. Shapira, S. Foner, D. H. Ridgley, K. Dwight, and A. Wold, *Phys. Rev. B* **30**, 4021 (1984).

⁴R. L. Aggarwal, S. N. Jasperson, Y. Shapira, S. Foner, T. Sakakibara, T. Goto, N. Miura, K. Dwight, and A. Wold, in *Proceedings of the Seventh International Conference on the Physics of Semiconductors, San Francisco, 1984*, edited by J.

D. Chadi and W. A. Harrison (Springer-Verlag, Berlin, 1985), p. 1419.

⁵R. L. Aggarwal, S. N. Jasperson, P. Becla, and R. R. Galazka, *Phys. Rev. B* **32**, 5132 (1985).

⁶G. Bastard and C. Lewiner, *Phys. Rev. B* **20**, 4256 (1979).

⁷C. Lewiner and G. Bastard, *J. Phys. C* **13**, 2347 (1980).

⁸Ven-Chung Lee and L. Liu, *Phys. Rev. B* **29**, 2125 (1984).

⁹S. Takeyama and S. Narita, *Jpn. J. Appl. Phys.* **24**, 1270 (1985); *J. Phys. Soc. Jpn.* **55**, 274 (1986).

¹⁰N. Miura, G. Kido, H. Miyajima, K. Nakao, and S. Chikazumi, in *Physics in High Magnetic Fields*, edited by S. Chikazumi and N. Miura (Springer, Berlin, 1981), p. 64.

¹¹N. Yamada, S. Takeyama, and N. Miura (unpublished).

- ¹²S. Nagata, R. R. Galazka, D. P. Mullin, H. Akbarzadah, G. D. Khattak, J. K. Furdyna, and P. H. Keesom, *Phys. Rev. B* **22**, 3331 (1980); R. R. Galazka, S. Nagata, and P. H. Keesom, *Phys. Rev. B* **22**, 3344 (1980).
- ¹³D. Heiman, Y. Shapira, S. Foner, B. Khazai, R. Kershaw, K. Dwight, and A. Wold, *Phys. Rev. B* **29**, 5634 (1984).
- ¹⁴D. Heiman, Y. Shapira, and S. Foner, *Solid State Commun.* **45**, 899 (1983).
- ¹⁵A. Wittlin, M. Grynberg, W. Knap, J. Kossut, and Z. Wilamowski, in *Proceedings of the Fifteenth International Conference on the Physics of Semiconductors, Kyoto, Japan, 1980* [*J. Phys. Soc. Jpn. A* **49**, 635 (1980)].
- ¹⁶S. Hikami, A. I. Larkin, and Y. Nagaoka, *Prog. Theor. Phys.* **63**, 707 (1980).
- ¹⁷Y. Shapira, S. Foner, and N. F. Oliveira, Jr., *Phys. Rev. B* **10**, 4781 (1974).